Case Study: Development of a Biaxial Tensile Testing Machine for Soft Materials and Biological Tissues

Reuben A. Govender[a] and Jonathan A. Caine [b]

Received 30 January 2025, in revised form 17 February 2026 and accepted 21 July 2026

Abstract: While uniaxial tensile testing machines are ubiquitous, very few local institutions have access to biaxial tensile testing facilities, and even fewer have machines suited for low-force applications such as elastomers or biological tissues. This case study reports on the design of a custom planar biaxial tensile testing machine, which functioned as a stand-alone desktop tensile tester with two independent, orthogonal testing axes to facilitate the investigation of soft biological materials. Two $50\,\mathrm{N}$ ***load cells were used to measure load, and a non-contact Digital Image Correlation system was used to measure three-dimensional surface displacement. Commissioning testing was performed using a silicone elastomer (Smooth-On, Dragon Skin 10) which served as a surrogate for skin. The testing did not seek to characterise the surrogate material, but to verify that the machine operated as intended. Tensile specimens were tested on the custom machine and a commercial tensile testing machine for comparison at four crosshead displacement rates:*** $10, 50, 120$ ***and*** $400\,\mathrm{mm\,min^{-1}}$***. Planar biaxial tensile testing was then performed on cruciform Dragon Skin 10 specimens at the same speeds, but at different speed ratios between the testing axes. The performance of the custom-built machine was critically assessed, and the areas of difficulty encountered during testing were handling and gripping highly pliable specimens, maintaining consistent specimen boundary conditions, and ensuring alignment. The testing demonstrated that the machine functioned as intended and met the requirements for use in testing skin and other membrane tissues in the future.***

Additional keywords: Biological Materials, Biaxial Tension, Digital Image Correlation

1 Introduction

Biaxial tensile testing is essential for the mechanical characterisation of thin materials (membranes) that exhibit some anisotropy, as uniaxial tests alone provide insufficient information to accurately determine constitutive model parameters. This is particularly true for Biological Membrane Tissues (BMT), where scarcity of specimens and heterogeneity make it problematic to harvest multiple specimens at differing angles for uniaxial tensile testing. Despite the long-standing use of biaxial testing in international research [1, 2, 3], biaxial tensile testers of any scale are not readily accessible to South African researchers. There are commercially available biaxial tensile testers designed for biological tissue, such as the CellScale BioTester™(Waterloo, Canada). However, the capital cost of such platforms is prohibitive, and deformation instrumentation for these machines lags behind modern techniques such as Digital Image Correlation (DIC). This project aimed to design, build, and commission a Planar Biaxial Tensile Tester (PBTT) suitable for soft specimens such as biological membranes, incorporating Digital Image Correlation measurements that were not available with commercial biaxial testers.

There is no standardised method for testing the mechanical properties of biological membrane tissues, though standard test methods do exist for metals [4]. Mechanical testing of BMT can be separated into two broad categories: *in vivo* testing and *in vitro* testing. *In vivo* testing has the advantage of testing BMT in its natural state in the donor organism, avoiding degradation and any changes due to environmental conditions. It is difficult to separate the BMT response from that of the surrounding connective tissue in the donor organism. Hence, *in vivo* methods are not well suited for mechanical characterisation studies, particularly where testing the tissue to failure would cause harm to the donor.

Unlike *in vivo* testing, *in vitro* testing requires that the tissue be excised from the donor and that measurements be conducted on a separate testing platform. *In vitro* testing provides well-defined boundary conditions for the specimen, which is important for fitting constitutive models. However, *in vitro* testing carries the unavoidable risk of damaging the tissue during excision. The tissue will begin to degrade once removed from the host organism, and additional measures are required for the testing environment to closely mimic the *in vivo* conditions. This motivated the design requirement that the testing hardware be portable and could be mounted on any desktop, such that the biaxial tester could be relocated to a laboratory close to where biological specimens were harvested, to minimise the opportunities for degradation of tissue specimens during storage and transport.

Due to the very compliant, fragile nature of BMT, traditional methods of deformation or strain measurement, such as Linear Variable Differential Transformers (LVDT) or strain gauges, are not suitable, as these alter the local stiffness or boundary conditions of the specimen. Prior research has re-

[a] ORCID 0000-0002-1428-4142. Department of Mechanical Engineering, University of Cape Town. Private Bag X3, Rondebosch, 7701, South Africa. E-mail: reuben.govender@uct.ac.za

[b] ORCID 0000-0003-0777-7800.Department of Mechanical Engineering, University of Cape Town.

http://dx.doi.org/10.69694/2309-8988/2026/v42a2
http://www.saimeche.org.za (open access) © CC BY 4.0

lied on optical tracking of markers, painted onto the specimen [2, 5], facilitating non-contact deformation measurements. However, these studies and more recent commercial platforms such as the CellScale BioTester™have relied on tracking a small number (typically four or five) of discrete dots in a cruciform array. The specimen strain was inferred using the planar displacement of the dots and a finite difference approximation. This yields averaged values for strain for the two perpendicular tension directions and one shear strain. Dot tracking, at this scale, does not provide any information on variation or localisation of strain across the specimen.

DIC is also a non-contact, optical measurement of deformations, but it can provide deformation measurements over the "full field" of the specimen. DIC achieves this by tracking subsets of pixels over the entire specimen, rather than a small number of discrete markers. DIC requires that the specimen surface have a randomised speckle pattern, allowing adjacent sub-sets of pixels to have distinct grayscale distributions that can be tracked from image to image [6]. The spatial resolution of measurements is limited by a combination of speckle size distribution, speckle contrast and the camera characteristics. By using two or more cameras to provide stereo vision, DIC is regularly extended to 3D deformations, where older dot-tracking methods are typically limited by a planar deformation assumption.

This article will describe the design of the custom Planar Biaxial Tensile Tester that incorporates DIC deformation measurement. The article includes the motivation for key design decisions and an evaluation of the performance of the PBTT during commissioning testing, using silicone elastomer specimens as a surrogate for soft biological tissue. The general layout of the PBTT is shown in Figure 1. For more detailed schematics and engineering drawings, the reader is referred to [7].

2 Design of Apparatus

2.1 Requirements

The requirement that drove most decisions was for the PBTT to apply a load of up to 50 N in perpendicular directions on a plane. A review of experimental studies on skin and similar membrane tissues [3, 8, 9, 10, 11] indicated that peak forces were unlikely to exceed 50 N. Given that the CellScale Bio™, a commercially available biological material tester, had a maximum capacity of 23 N, the chosen design load of 50 N would allow some flexibility for testing stronger tissues without placing an onerous requirement for component loading.

Specimen dimensions would be limited to 50 x 50 mm. Where biological tissue specimens are available in larger dimensions, the inherent variability of biological tissue introduces complications. Hence, designing for a larger specimen had limited utility. The maximum intended strain rate of $0.1\,\mathrm{s}^{-1}$, which is the upper bound of the quasi-static regime, along with a gauge length of 50 mm, sets the target deformation rate of $300\,\mathrm{mm\,min}^{-1}$. This target was increased to $400\,\mathrm{mm\,min}^{-1}$ to ensure some safety margin on any machine dynamic effects.

2.2 Deformation and Strain Measurement

Full field 3D deformations of the specimen were obtained using 3D DIC. Biological specimen surfaces have larger variations in flatness than metals or polymers, and mounting inaccuracies were anticipated. Using a single camera, the 2D DIC system does not permit any measurement of out-of-plane variation. Using stereo cameras and obtaining 3D measurements permitted interrogation of any out-of-plane displacement, whether this was due to inherent specimen variability or imperfect mounting. Stereo images were captured using 5 MP cameras and processed using Dantec Dynamics ISTRA4D DIC software, which was available for use in the laboratory at no additional cost to this project.

The DIC system is a standalone system, with the only connection between the DIC system and the custom PBTT being an analogue connection, which sends load cell force data to the DIC system. This ensures the force and DIC data are synchronised correctly with the force data from the load cells and can be analysed together on the Dantec ISTRA4D software in post-processing. The frame rate of the cameras was adjusted according to the crosshead speeds, with 5 frames per second at the lower speed and 25 frames per second at the highest speed.

The decision to use DIC for deformation measurements was made at project inception and was factored into other design decisions such as the actuator layout (Section 2.4) and control system (Section 2.5).

2.3 Frame Design

Traditional material testing frames utilise precision-machined and ground components to maximise rigidity, in the context of kilo-Newton-scale loads and sub-millimetre specimen deformations. Given the load limit of 50 N and grip speeds of $400\,\mathrm{mm\,min}^{-1}$, the PBTT has more in common with 3D printer platforms in terms of loads and speeds than a testing frame for metallic specimens. Hence, the conceptual design of this apparatus drew inspiration from various 3D printer platforms, which utilise extruded aluminium beams as both machine structure and motion guides, along with stepper motors receiving G-Code as an open-loop motion control system. Applying similar design choices to the PBTT reduced manufacturing time and costs and increased flexibility for later design changes, allowing a functional prototype to be built and tested.

2.4 Linear Actuation and Machine Layout

The linear actuators would ultimately be lead screws driven by stepper motors, a choice commonly found in commercial test frames. The requirement for portability, the low design force requirements and ease of implementation of position control motivated against pneumatic or hydraulic actuation. Typically, on a uniaxial tensile testing machine, one end of the specimen is clamped in a stationary grip, with the other end mounted in a grip on a movable cross-head (single grip displacement). This means the centre of the specimen moves relative to a stationary observer.

http://dx.doi.org/10.69694/2309-8988/2026/v42a2
http://www.saimeche.org.za (open access) © CC BY 4.0

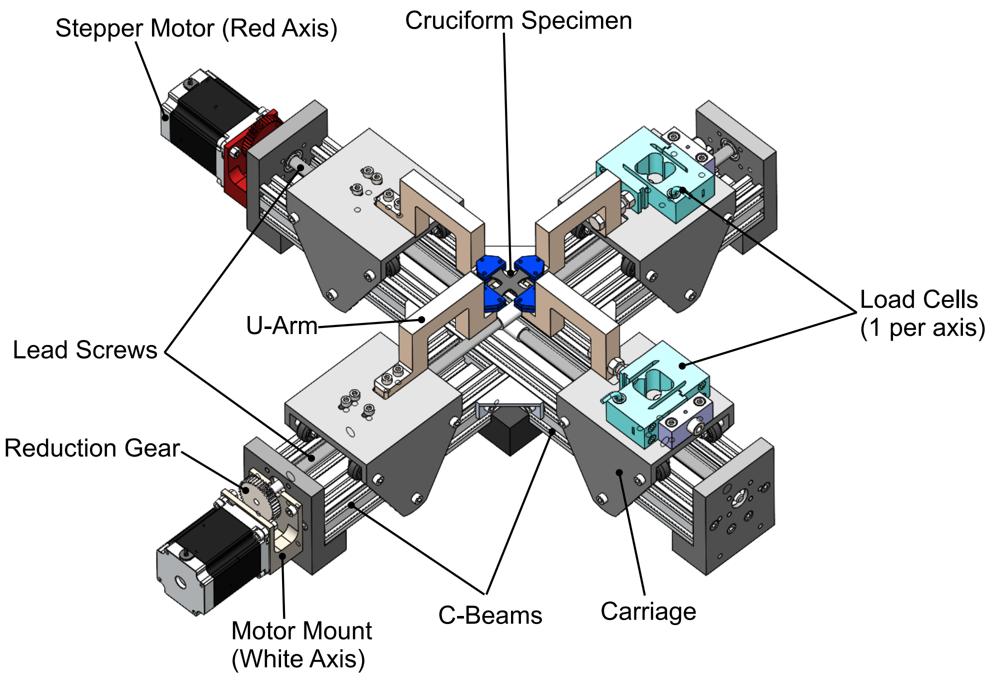

Figure 1 CAD Model of Planar Biaxial Tensile Tester

If a biaxial tensile testing machine keeps two adjacent grips stationary while the opposite grips move, the cruciform specimen deforms in a non-symmetric manner. However, if both grips on an axis displace symmetrically in opposite directions, the specimen's deformation is symmetric and more uniform in the region of interest. This is demonstrated in Figure 2, using Finite Element (FE) simulations* with relevant boundary conditions for (a) single grip displacement and (b) symmetric dual grip displacement. Furthermore, keeping the region of interest centred is desirable for image-based deformation measurements, as the position will remain stationary relative to the optical deformation measurement device.

Meeting the desired kinematics requires four moving grips as opposed to the single moving grip found on typical uniaxial tensile testing machines. This adds significant complexity to the design when compared to a uniaxial tensile testing machine. The custom machine was designed such that both carriages on a single axis are powered by the same motor and are mechanically coupled.

Without mechanical coupling of the carriages, separate electrical drives on the same axis would need closed-loop control to avoid having different displacements or speeds on the same axis. Therefore, carriages on the same axis were mechanically coupled to mitigate any errors that may arise due to the carriages on a single axis not moving in unison.

The custom PBTT consists of two carriages on the same axis, which are connected to the same lead screw. Each axis has a stepper motor which drives the lead screw via a gear reduction. Half of the lead screw has a left-handed thread, and the other half has a right-handed thread, as shown in the concept sketch in Figure 3(a). As the lead screw is rotated by the stepper motor, the opposite threads ensure the two carriages move an equal distance in opposite directions along the same axis, achieving the desired specimen boundary conditions. The lead screw was fabricated by joining two lengths of right- and left-hand trapezoidal lead screw stock (Igus Dryspin®10 mm outer diameter, 3 mm pitch, single start, Stainless Steel 304) using a shrink fit sleeve.

The main structure of the machine, shown in Figure 1, consists of extruded aluminium C-beams with V-slots and doubles as the carriage guide system. Each partially constrained carriage moves along the C-Beam via six V-wheels that interface with the V-slots of the C-beam, as shown in Figure 3(b). The guide system interfaces with the linear actuation system on either end of the C-beam extrusion by a fixed end-plate, which houses the lead screw bearings, fully constraining the system. The carriages are connected to the lead screw via the anti-backlash nuts, which minimise discrepancies in displacement of the carriages when there is a direction change in the motion of the carriages. The carriages are constrained by the wheels so that they can only move axially along the deformation axes, and all other motion is constrained.

The wheel and carriage arrangement was preferred over linear bearings due to the (relatively) large toppling moments, as the specimen plane and hence tensile forces are offset from the lead screw axes. The wheel positions could be fine-tuned using eccentric bushings to reduce any play due to manufacturing tolerances. Furthermore, the V-wheels could run directly in the slotted aluminium extrusions, while any linear bearing system would have required additional guide rails to be mounted on the frame.

*The FE simulation used a linear elastic material with an arbitrarily low modulus for illustrative purposes

http://dx.doi.org/10.69694/2309-8988/2026/v42a2
http://www.saimeche.org.za (open access) © CC BY 4.0

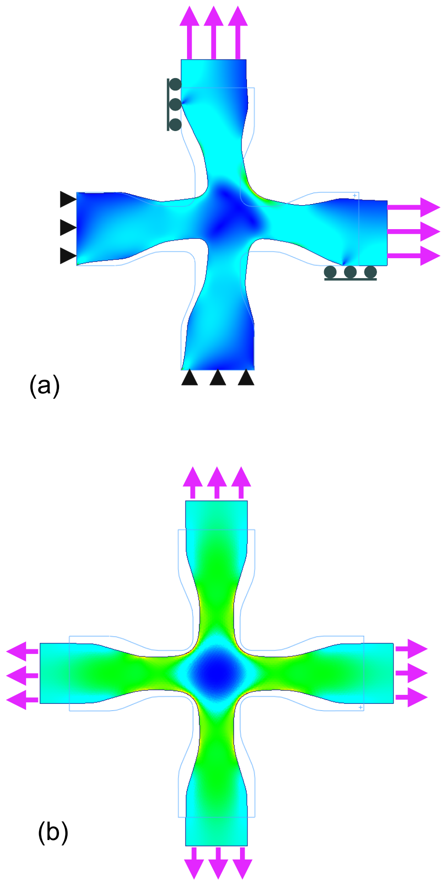

Figure 2 Principal strains of FE simulation of cruciform biaxial specimen subjected to (a) single grip moving per axis; (b) symmetric dual grip movement

2.5 Control and Force Instrumentation

While the "gold standard" for materials testing is a closed-loop control system that can hold either displacement or force at constant rates specified by the user, this was not considered essential for the first prototype in this application. Specimen deformations would be measured using DIC, which is post-processed and therefore does not yield displacement data at a suitable rate for a control loop. Implementing closed-loop control would require integrating an additional set of displacement instruments, adding to the development time. Instead, the use of open-loop displacement control using G-Code instructions, as used on many desktop 3D printers, was considered sufficient for the first prototype.

The control system runs on an Arduino Uno microcontroller, coupled to a Grbl shield. Grbl[†] is an open-source motion control system [12], originally designed to use open-loop control and stepper motors to run CNC devices, that can be run on an Arduino Uno microcontroller. The Grbl shield is equipped with DRV8825 stepper motor drivers to control each axis, which is driven by a Wantai, 1 N m NEMA-17 stepper motor. Motion instructions are sent to the Arduino as G-code using Universal G-Code Sender - an open-source software used for interfacing with CNC controllers. For simple, monotonic extension tests, the user only needed to specify a rate and distance on the G-code sender.

For tests where more complex motion was desired, such as differing extensions on each axis or cyclic deformation, these are easily implemented as G-code and uploaded to the machine for execution.

Each axis of the machine was equipped with two limit switches: one to indicate a "home position" (corresponding to nominally zero extension) and the second to indicate the carriage had reached maximum extension. While the GCode Sender interface included software stop buttons, a hardware "Emergency Stop" button was wired in to cut power to both stepper motors, causing the machine to stop in position.

A single axial load cell on each axis was used to measure the axial load applied through the specimen. Two 50 N HBM (Hottinger Baldwin Messtechnik, Darmstadt, Germany) K-S2M tensile load cells were purchased along with two HBM ClipX devices. The ClipX is a combined load cell amplifier and signal conditioner which connects to a PC via an Ethernet connection, set to sample data at 100 Hz. The load cell is slightly raised from the carriage and interfaces with a U-shaped "arm" which has a modular interface to connect with the grips. The arm has a U shape, seen in Figure 3(b), to allow the specimen to be immersed in saline solution if needed.

3 Testing Methodology

The performance of the custom PBTT was critically assessed by comparison with data obtained from a commercially manufactured and calibrated tensile test machine. Due to the lack of access to a commercially built biaxial tensile tester, a uniaxial testing machine was used. Therefore, each axis of the custom machine was tested individually as a uniaxial tensile testing machine for the comparative study. The commercial machine was an Instron testing machine with a 100 N load cell and a resolution of 0.001 N, at the Centre for Materials Engineering at the University of Cape Town. Deformation measurements for both the custom machine and Instron were performed using the DIC system. Only once the performance of each axis of the custom-built machine had been proven to be adequate were full biaxial tensile tests performed.

Dragon Skin 10 (Smooth-On) silicone elastomer was chosen as the skin surrogate for all testing. Dragon Skin 10 is a Shore 10A platinum-cure liquid silicone compound predominantly used for special effects in the film and entertainment industries. It was chosen as it has a similar modulus to that of skin in the toe region, it is also highly pliant (1000% elongation at break [13]), it is readily available and easy to use and presents no chemical or biohazard safety concerns. Specimens were cast in a laser-cut acrylic mould. For the uniaxial tension tests, the specimen dimensions were based on ASTM D412 [14], which is a standard test method for rubber and elastomeric materials. Biaxial tension specimens followed a cruciform shape, with dimensions shown in Figure 4(a). The specimens were cast with a white background, with a black speckle pattern applied while the substrate was partially cured, as seen in Figure 4(b).

[†] Grbl is not an acronym and is pronounced "gerbil" according to the original author.

http://dx.doi.org/10.69694/2309-8988/2026/v42a2
http://www.saimeche.org.za (open access) © CC BY 4.0

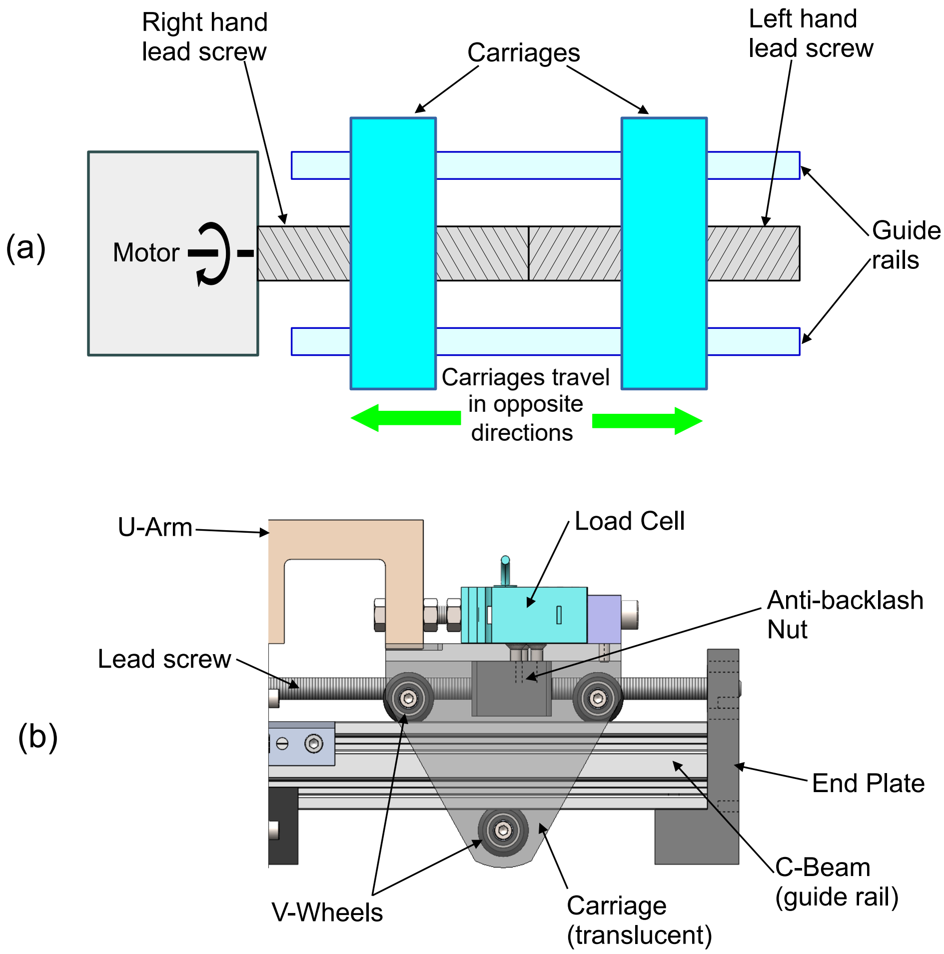

Figure 3 (a) Schematic top view of leadscrew and carriage layout (b) CAD side view of carriage wheel supports

This speckle-pattern allowed the specimens' surface deformation to be recorded using DIC. The black speckle pattern was made using a liquid silicone-based paint (Smooth-On Psycho Paint ™[15]) which was applied to the specimens using an airbrush. The black speckles were sprayed on when the white substrate was partially cured, to balance the competing requirements of good adhesion and minimising colour bleed and associated blurring of speckles. This method was able to provide the consistently fine speckle pattern needed when working with such small specimens (dog bone specimens with a gauge area of 5 x 20 mm). Specimens were mounted using compression clamp grips, which could pivot on each arm to reduce the effects of misalignment. A gripping system which is suited to delicate BMT was left for future work.

Tests were performed at 50 and 400 mm min^{-1} on both axes of the custom machine and the Instron uniaxial testing machine. At least 5 samples were tested at each speed on each axis. Both systems used the same DIC system (Dantec) and cameras to record the surface deformation of the specimens. Engineering stress versus engineering strain graphs were generated for all samples to allow the performance of the two machines to be compared.

Biaxial tensile tests were performed, but no reference data was available for comparison. Fitting the biaxial data to a hyperelastic constitutive model was outside the scope of this study. The biaxial tensile tests helped assess the functionality of the custom machine and the quality of data obtained. Cross-head speeds and ratios were varied for the different tests to ensure the machine could work over a wide range of speeds similar to what would be used in the testing of soft tissues. A cross-head speed ratio of 1:1 would equate to both axes running at the same speed, and a 1:0 ratio would mean one axis running at the selected speed, while the other is held stationary. There were 4 speeds (10, 50, 120 and 400 mm min^{-1}) and 4 ratios (1:1, 1:0.75, 1:0.5, and 1:0) used for testing; providing a total of 20 different possible tests. Some test conditions were run multiple times to assess repeatability, though each specimen was only used once. A subset of the testing results is presented in this article for brevity, and the reader is referred to [7] for the complete results.

http://dx.doi.org/10.69694/2309-8988/2026/v42a2
http://www.saimeche.org.za (open access) © CC BY 4.0

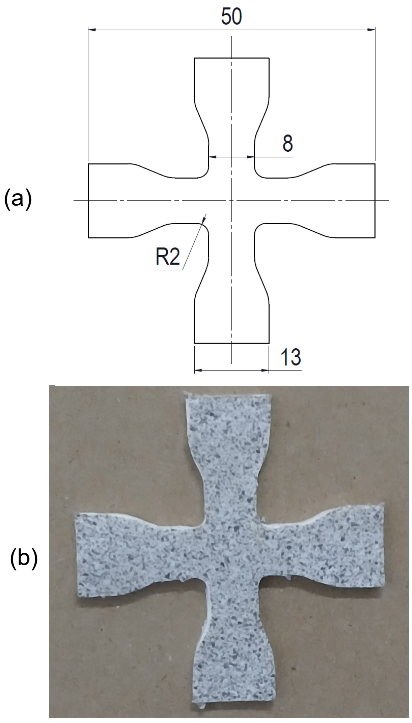

Figure 4 Biaxial tension cruciform specimens (a) Specimen schematic, dimensions in mm (b) Cast and speckled specimen

4 Results

4.1 Crosshead Displacement and Speed Testing

As the custom PBTT ran in open-loop displacement control, it was important to verify that the crossheads were moving as intended. The carriages were commanded to each move outwards 15 mm, for a total extension of 30 mm, using G-Code commands. The carriage displacement was measured using a Vernier calliper and confirmed to be ≤ 0.1 mm for all tests at a range of speeds. As specimen deformation was measured independently using DIC, this was deemed sufficient. The next phase of cross-head speed testing was conducted with a uniaxial test specimen in place and using DIC to measure specimen deformation. DIC was used to track points close to the grips, where there was negligible specimen strain, thereby providing a close approximation to the carriage motion as a function of time. Figure 5 shows the crosshead speed histories under load as determined from the DIC data, for tests at (a) 50 mm min^{-1} and (b) 400 mm min^{-1}.

The cross-head maintained a nominally constant speed, close to the set point, with some visible variation. It was not clear whether this variance was due to noise on the DIC measurements or actual short-duration changes in cross-head speed. However, it was apparent that the open-loop control was capable of holding an acceptably uniform speed at the normal operating loads. Reducing these small variations would require additional displacement instrumentation and a closed-loop control system, which did not represent sufficient benefit for the broader project aims, compared to moving ahead with open-loop control.

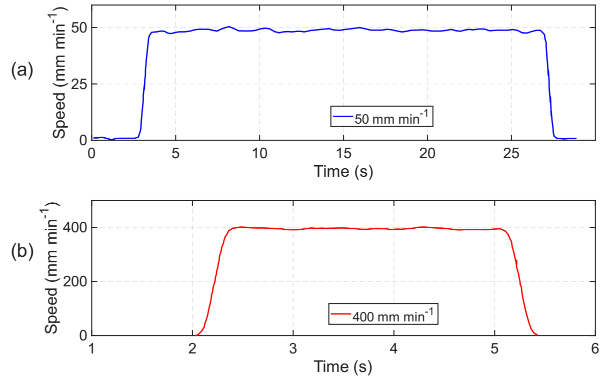

Figure 5 Cross head speed histories at (a) 50 mm min^{-1} and (b) 400 mm min^{-1}

4.2 Uniaxial Tensile Testing

The two axes of the custom PBTT are listed as the Red Axis and the White Axis. Data obtained from testing on the Instron machine is simply listed as Instron. It must be noted that there was some difficulty placing the extremely flexible specimens into the grips fitted onto the Instron machine, and it is expected that this is responsible for some of the variation recorded during the Instron machine tests. Difficulty handling the small pliable specimens is also a challenge reported widely in the literature when testing soft tissues [11, 16]. Figure 6 compares the engineering stress-strain response for all tests performed at 50 mm min^{-1} (on the Instron and PBTT's White axis and Red axis). The green solid band is the bounds of all data tested on the Instron at 50 mm min^{-1}. Note that the dual lines for the PBTT's data are upper and lower limits for loading curves, not an averaged load-unload test.

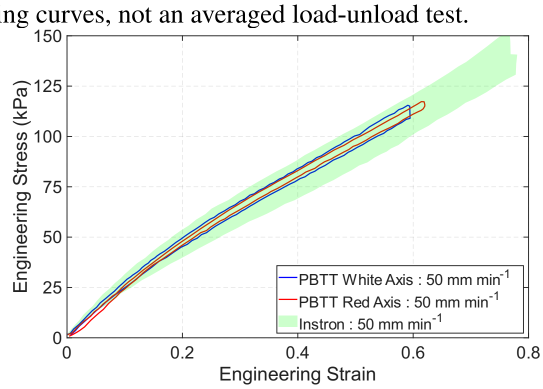

Figure 6 Comparison of uniaxial tension results at 50 mm min^{-1}

Figure 7 compares the uniaxial engineering stress-strain response, as measured by the Instron and the custom PBTT's White and Red axes, at a crosshead speed of 400 mm min^{-1}. The results shown in Figure 6 and 7 have been limited to a strain below 70%, as the custom PBTT was not designed for such large specimens and deformations as the Instron machine. The specimen size and expected deformations of biological biaxial specimens are significantly smaller than those used during this comparative study, hence the PBTT travel limits should suffice.

It is clear that the stress-strain data measured by the custom PBTT machine lie within the bounds of the data measured on the Instron, for both speeds tested. The custom machine force

http://dx.doi.org/10.69694/2309-8988/2026/v42a2
http://www.saimeche.org.za (open access) © CC BY 4.0

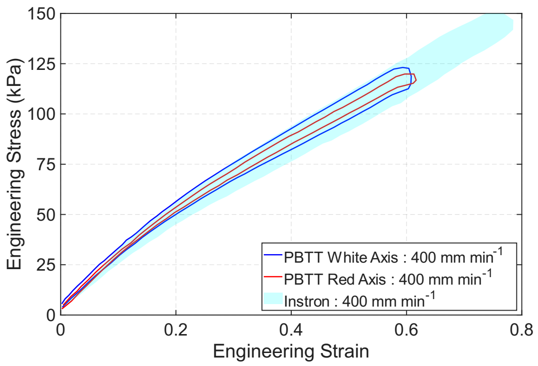

Figure 7 Comparison of uniaxial tension results at 400 mm min^{-1}

results were determined purely using the manufacturer's provided calibration factor, without any filtering. These results provided confidence that the custom machine's force measurements on both axes were accurate. Comparison of the stress-strain response at both speeds shows a slightly stiffer response at 400 mm min^{-1}, which would be consistent with the elastomer specimens having some viscous response. However, the rate sensitivity of this specific silicone elastomer was not of interest at this stage of the project.

4.3 Biaxial Tensile Testing

After successfully completing the uniaxial comparative testing, planar biaxial testing was performed using the custom PBTT. Cruciform specimens were used, with sufficiently long arms that clamping stresses do not affect the central gauge section. A downside of the cruciform geometry is that it is not possible to calculate a representative true stress for the gauge section due to the changes in cross-section. The force per unit width of the arms is reported instead. Figure 8 shows the cruciform specimen, mounted in the PBTT.

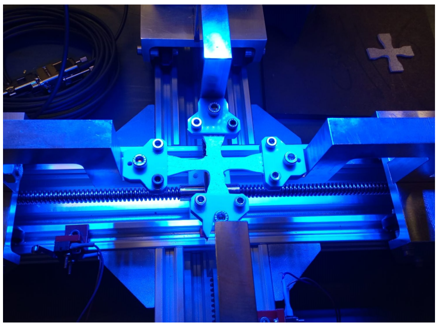

Figure 8 Cruciform specimen mounted in biaxial tensile tester

Initial biaxial tests were conducted at equal deformations on both axes, at speeds ranging from 10 to 400 mm min^{-1}. The principal engineering strain was post-processed using the Istra4D DIC software, and a representative sample is shown in Figure 9. The strain field is as expected, with the quivers denoting the direction of the maximum principal strains aligning with the arms. The average strain in each arm is similar for both X- and Y-axes.

The force per unit thickness for all equi-biaxial tests, across a range of speeds, is plotted as a function of engineering strain

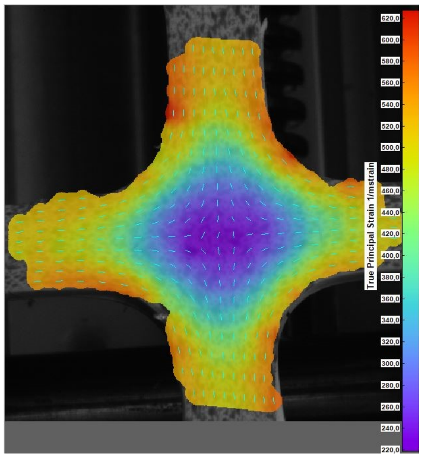

Figure 9 Principal engineering strain for equi-biaxial deformation

(averaged over the gauge section) in Figure 10. There is minimal variation between each axis for any given test. While the PBTT is capable of exerting and measuring compression on either axis, large compressive deformation would cause a compliant membrane to buckle. Further biaxial tests were conducted with varying tensile deformation ratios (1:0.5 and 1:0), that avoided excessive compression.

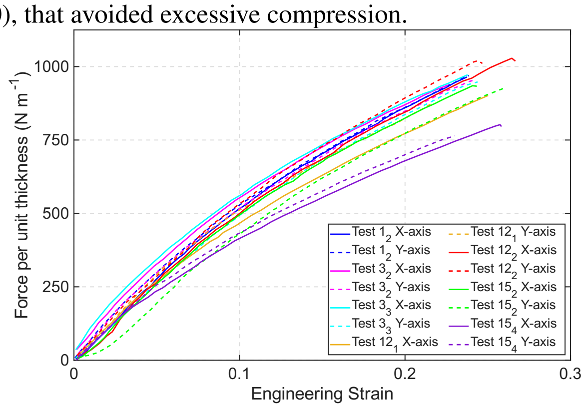

Figure 10 Force per unit thickness for equi-biaxial deformation

The principal strain field for a deformation ratio of 1:0.5, where the X-axis is traversed at 400 mm min^{-1} while the Y-axis is traversed at 200 mm min^{-1}, is shown in Figure 11. The strains in parallel arms have similar distributions and are practically equal. The strains in the X-axis arms are significantly larger than those in the Y-axis arms, as expected, though not precisely equal to the deformation ratio. The strains in the Y-axis are smaller than half of the X-axis strains, because Poisson contraction effects from the larger X-axis deformations are counteracting the applied deformation in the Y-axis.

The force per unit thickness for all tests at a 1:0.5 deformation ratio, across a range of speeds, is plotted in Figure 12. The loads in the Y-axis are smaller than the X-axis, which aligns with expectations, as less deformation is being applied to the Y-axis. Tests were performed at a deformation ratio of 1:0. This is not the same as a uniaxial test, as the Y-axis arms provide some lateral restraint. The force/unit thickness response for the 1:0 deformation ratio is plotted in Figure 13.

http://dx.doi.org/10.69694/2309-8988/2026/v42a2
http://www.saimeche.org.za (open access) © CC BY 4.0

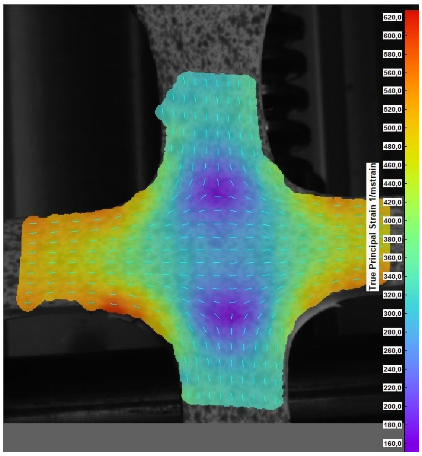

Figure 11 Principal engineering strain for 1:0.5 deformation ratio

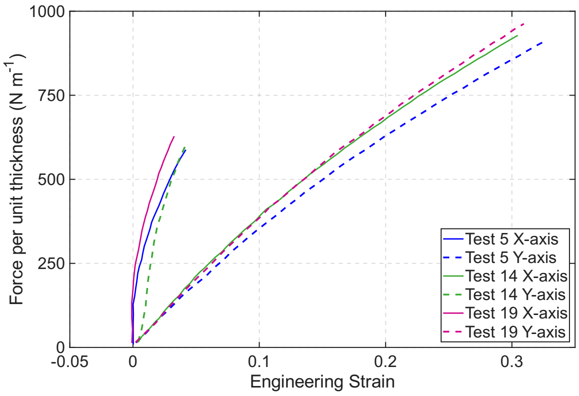

Figure 12 Force per unit thickness for 1:0.5 deformation ratio

While both axes exhibit tensile stress, the engineering strain in the Y-axis is negative. This is consistent with Poisson contraction effects from the much larger X-axis deformations, while the stationary Y-axis grips provide sufficient restraint to develop tensile stress. The mounting of very flexible elastomer specimens proved to be challenging and required close attention by the operator. A metal or more rigid polymer specimen can be mounted horizontally with little sag, and the application of significant preload to the specimen would be easily detected. However, for very flexible elastomers, it is not straightforward to determine how much pre-tension has been applied while ensuring the specimen slack has been taken up.

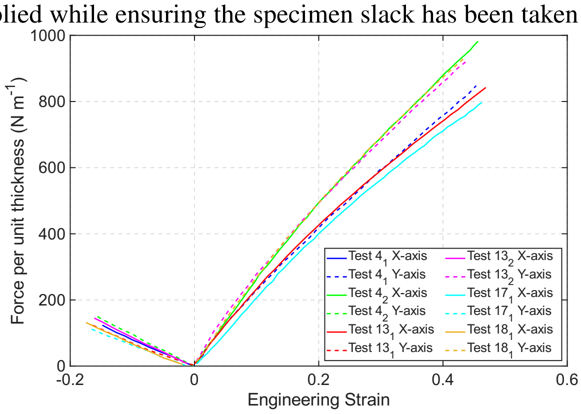

Figure 13 Force per unit thickness for 1:0 deformation ratio

If the mounting clamps are not free to rotate due to an assembly error, unintended loads may be applied to the specimen. Figure 14 shows a specimen which was accidentally misaligned during mounting before being subjected to equi-biaxial tension.

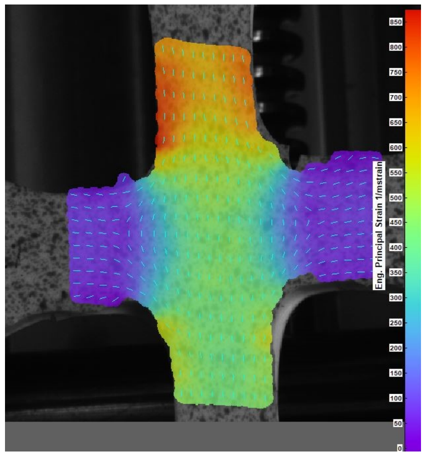

Figure 14 Incorrectly mounted specimen

The principal strain distribution shows significant differences between the upper and lower arms, which should be nominally equal. The left and right arms, while having low strain values, show significant misalignment under full tension that was not visible at the start of the test. This emphasises the importance of correct mounting procedure, but also the ability of DIC to highlight problems that would be masked if using strain gauges or other instruments to measure specimen deformation.

5 Concluding Remarks

A Planar Biaxial Tester suited for soft, compliant specimens was designed and manufactured. The PBTT's capabilities were demonstrated, using silicone elastomer specimens. For purely uniaxial tensile tests, the engineering stress-strain data yielded by the custom PBTT compared well with data from tests performed on an Instron machine. The PBTT data lay within the scatter of the Instron data for any given crosshead speed, which is promising given that the maximum forces are typically below 10 N.

For low-stiffness specimens such as elastomers, the mechanical advantage and the stepper motor torque proved sufficient for maintaining a constant crosshead speed without requiring closed-loop control. The DIC deformation measurements produced full-field strain data, which provides for richer future investigations over commercial PBTT solutions that rely on discrete marker tracking and hence provide only a single average value for the strain in each axis.

The PBTT could be set to different deformations on each axis by simply modifying G-Code commands for the independent stepper motors driving each axis. Biaxial tensile tests, using cruciform elastomer specimens, yielded sensible data. As deformation ratios were changed from equi-biaxial deformation to zero imposed deformation on the transverse axis, the Poisson contraction effects of the primary axis' deformation became more apparent. The tests performed on the PBTT

http://dx.doi.org/10.69694/2309-8988/2026/v42a2
http://www.saimeche.org.za (open access) © CC BY 4.0

demonstrated that it should be capable of testing biological tissues at the loads and strains anticipated. Developing a robust gripping system and mounting methodology that will be suitable for biological tissues, that are typically more compliant and sensitive to lateral deformations, is left for future development of the PBTT.

Acknowledgements

This research was supported financially by the National Research Foundation of South Africa, via Thuthuka Grant UID 113361, held by R.A. Govender. The authors are grateful for the input of the UCT Mechanical Engineering Workshop staff in machining and fabrication of hardware, and the helpful suggestions of A.M. Graham and A.M. Curry regarding speckling elastomer specimens.

References

[1] Y. Lanir and Y.C. Fung. Two-dimensional mechanical properties of rabbit skin I: Experimental system. *Journal of Biomechanics*, 7(1):29–34, 1974. doi: https://doi.org/10.1016/0021-9290(74)90067-0.

[2] M.S. Sacks. Biaxial mechanical evaluation of planar biological materials. *Journal of Elasticity and the Physical Science of Solids*, 61(1):199–246, 2000. doi: https://doi.org/10.1023/A:1010917028671.

[3] J.S. Grashow, A.P. Yoganathan, and M.S. Sacks. Biaxial stress-stretch behavior of the mitral valve anterior leaflet at physiologic strain rates. *Annals of Biomedical Engineering*, 34(2):315–325, 2006. doi: https://doi.org/10.1007/s10439-005-9027-y.

[4] British Standards Institution. BS ISO 16842: Metallic materials - Sheet and strip - Biaxial tensile testing method using a cruciform test piece, 2021. URL `https://www.iso.org/standard/82087.html`.

[5] M.S. Sirry, J.R. Butler, S.S. Patnaik, B. Brazile, R. Bertucci, A. Claude, R. McLaughlin, N.H. Davies, J. Liao, and T. Franz. Characterisation of the mechanical properties of infarcted myocardium in the rat under biaxial tension and uniaxial compression. *Journal of the Mechanical Behavior of Biomedical Materials*, 63:252–264, 2016. doi: https://doi.org/10.1016/j.jmbbm.2016.06.029.

[6] M.A. Sutton, J.J. Orteu, and H. Schreier. *Image correlation for shape, motion and deformation measurements: basic concepts, theory and applications*. Springer Science & Business Media, 2009. ISBN 9780387787473.

[7] J.A. Caine. Design, build and test of a planar biaxial tensile testing machine for skin and other collagenous soft tissues. MSc Thesis, University of Cape Town, 2022. URL `http://hdl.handle.net/11427/37066`.

[8] A. Pissarenko, W. Yang, H. Quan, K.A. Brown, A. Williams, W.G. Proud, and M.A. Meyers. Tensile behavior and structural characterization of pig dermis. *Acta Biomaterialia*, 86:77–95, 2019. doi: https://doi.org/10.1016/j.actbio.2019.01.023.

[9] M.S. Sacks and D.C. Gloeckner. Quantification of the fiber architecture and biaxial mechanical behavior of porcine intestinal submucosa. *Journal of Biomedical Materials Research*, 46(1):1–10, 1999. doi: https://doi.org/10.1002/(SICI)1097-4636(199907)46:1%3C1::AID-JBM1%3E3.0.CO;2-7.

[10] A. Ní Annaidh, K. Bruyère, M. Destrade, M.D. Gilchrist, and M. Otténio. Characterization of the anisotropic mechanical properties of excised human skin. *Journal of the Mechanical Behavior of Biomedical Materials*, 5(1):139–148, 2012. doi: https://doi.org/10.1016/j.jmbbm.2011.08.016.

[11] M. Ottenio, D. Tran, A. Ní Annaidh, M.D. Gilchrist, and K. Bruyère. Strain rate and anisotropy effects on the tensile failure characteristics of human skin. *Journal of the Mechanical Behavior of Biomedical Materials*, 41:241–250, 2015. doi: https://doi.org/10.1016/j.jmbbm.2014.10.006.

[12] S.K. Jeon. *Grbl Wiki*, 2021. URL `https://github.com/grbl/grbl/wiki`.

[13] *Dragon Skin 10 Platinum Cure Silicon Rubber*. Smooth-On Products, 2021. URL `https://www.smooth-on.com/products/dragon-skin-10-nv/`.

[14] ASTM International. ASTM D412-16:2021 - Standard Test Methods for Vulcanized Rubber and Thermoplastic Elastomers—Tension, 2021. URL `https://store.astm.org/d0412-16r21.html`.

[15] *Pyscho Paint Silicon Paint*. Smooth-On Products, 2021. URL `https://www.smooth-on.com/products/psycho-paint`.

[16] M.S. Sacks and W. Sun. Multiaxial mechanical behavior of biological materials. *Annual Review of Biomedical Engineering*, 5(1):251–284, 2003. doi: https://doi.org/10.1146/annurev.bioeng.5.011303.120714.

http://www.saimeche.org.za (open access) © CC BY 4.0